

## RESEARCH COMMUNICATION

# In Vitro Biological Characterization of DCUN1D5 in DNA Damage Response

Wei Guo<sup>1</sup>, Guo-Jun Li<sup>4</sup>, Hong-Bo Xu<sup>1</sup>, Jie-Shi Xie<sup>2</sup>, Tai-Ping Shi<sup>2</sup>, Sheng-Zhong Zhang<sup>3</sup>, Xiao-Hong Chen<sup>1\*</sup>, Zhi-Gang Huang<sup>1\*</sup>

### Abstract

**Background:** Novel prognostic biomarkers or therapeutic molecular targets for laryngeal squamous cell carcinoma (LSCC) are an urgent priority. We here sought to identify multiple novel LSCC-associated genes. **Methods:** Using high-density microarray expression profiling, we identified multiple genes that were significantly altered between human LSCCs and paired normal tissues. Potential oncogenic functions of one such gene, DCUN1D5, were further characterized in vitro. **Results:** Our results demonstrated that DCUN1D5 was highly expressed in LSCCs. Overexpression of DCUN1D5 in vitro resulted in 2.7-fold increased cellular migration, 67.5% increased invasive capacity, and 2.6-fold increased proliferation. Endogenous DCUN1D5 expression was decreased in a time-dependent manner after genotoxic stress, and silencing of DCUN1D5 by siRNA decreased the number of cells in the S phase by 10.2% and increased apoptosis by 11.7%. **Conclusion:** Our data suggest that DCUN1D5 in vitro might have vital roles in DNA damage response, but further studies are warranted to assess its significance in vivo.

**Keywords:** DCUN1D5 - DNA damage - squamous cell carcinoma - larynx

*Asian Pacific J Cancer Prev*, 13, 4157-4162

### Introduction

Squamous cell carcinoma accounts for 90% of all malignancies of the larynx (Curado and Hashibe, 2009). LSCC progresses through multiple stages, each with distinct biologic and morphologic features (Leemans et al., 2005). As disease stage advances, chromosomal aberrations accumulate, resulting in a more aggressive cancer phenotype (Hermesen et al., 2005).

Like all head and neck cancers, LSCC shows a strong association with tobacco use, particularly cigarette smoking. Tobacco smoke can cause DNA damage that leads to cell-cycle deregulation, autonomous growth, and the development of invasive mechanisms, which result in carcinoma if the DNA damage is left unrepaired (Pfeifer et al., 2002; Mokhtar et al., 2011).

With use of high-density microarray profiling to screen for gene expression patterns in LSCC, we found that DCUN1D5 (DCN1, defective in cullin neddylation 1, domain containing 5) was particularly up-regulated in tumor samples of patients with LSCC who had a history of cigarette smoking. DCUN1D5, which has not been well studied, is located on chromosome 11q22.3. Amplification at chromosome 11q has been observed in several tumor types, most often in SCCs of mucosal origin, including those of the lung, head and neck, esophagus, and cervix. In these carcinomas, amplification at 11q was associated with

advanced tumor progression and an aggressive phenotype (Zhou et al., 2005; Parikh et al., 2007). DCUN1D5 cDNA encoded a protein of 237 amino acids, which contained two domains associated with DNA repair and cell cycle regulation (Kurz et al., 2005; Yang et al., 2007). Although no reported studies have clearly demonstrated DCUN1D5's role in cancer, one report suggested that DCUN1D5 expression may be useful as a biomarker for cervical cancer (Rajkumar et al., 2009).

Because DNA damage and repair pathways played critical roles in the development of LSCC, a smoking-related cancer, and because DCUN1D5 was found to be up-regulated in our patients with LSCC who had a tobacco history, we hypothesized that DCUN1D5 had a vital function involved in DNA damage response and repair in the carcinogenesis of LSCC.

### Materials and Methods

#### *Cell lines and tumor tissue*

HeLa (cervical adenocarcinoma) cells and Hep2 (LSCC) cells obtained from the American Type Culture Collection (ATCC) were cultured in RPMI 1640 medium with 10% fetal bovine serum (FBS). Primary laryngeal tumors and adjacent paired noncancerous normal tissues were collected from patients undergoing surgical resection at Beijing Tongren Hospital, after the patients provided

<sup>1</sup>Department of Otolaryngology-Head and Neck Surgery, Key Laboratory of Otolaryngology Head and Neck Surgery, <sup>2</sup>Department of Pathology, Beijing Tongren Hospital, Capital Medical University, <sup>3</sup>Department of Genomics, Chinese National Human Genome Center, Beijing, China, <sup>4</sup>Department of Head and Neck Surgery, The University of Texas M. D. Anderson Cancer Center, Houston, Texas \*For correspondence: [enthuangzhigang@sohu.com](mailto:enthuangzhigang@sohu.com), [entchenxiaohong@sohu.com](mailto:entchenxiaohong@sohu.com)

informed consent and the local ethics committee approved the study. Tissue samples were snap frozen in aliquots and stored in liquid nitrogen for gene microarray analysis.

#### Microarray analysis

A human genome oligonucleotide set (version 2.0) consisting of 5' amino acid-modified 70-mer probes and representing 21,329 well-characterized Homo sapiens genes was purchased from Operon. RNA from primary tumors and paired noncancerous normal tissues was isolated and reverse-transcribed to the cDNA. Quantification and normalization of intensity signals were performed using LuxScan 3.0 software (CapitalBio, China). Normalized log ratios of gene expression for all samples were imported into SAM software. Genes whose expression patterns were altered in LSCC were input into the EASE software under the "GO biological process" category of the Gene Ontology Consortium (Tusher et al., 2001; Cavalieri et al., 2007).

#### Reverse transcriptase polymerase chain reaction (RT-PCR)

The primers used for RT-PCR of DCUN1D5 were 5'-GCTAGACTAATAAGTGGAGAGGA-3' and 5'-CAGTCACACTGTAATGAAGTCAT-3'. The PCR designed to amplify the 242-bp fragment (386–628 bp) was performed at 94 °C for 5 min, 30 cycles of 94 °C for 30 s, 58 °C for 30 s, and 72 °C for 30 s followed by extension at 72 °C for 7 min. The relative fold increase of DCUN1D5 expression was determined by using glyceraldehyde-3-phosphate dehydrogenase (GAPDH) as a control.

#### Immunohistochemical analysis

Paraffin-embedded tissue samples were prepared for immunohistochemical analysis by anti-DCUN1D5 antibody (1:1000, Protein Tech Inc., China) using the immunohistochemical method, as described previously (Zhong et al., 2011).

#### Molecular cloning and subcellular localization

DCUN1D5-ORF was cloned into a pOTB7 vector (Protein Tech Inc., China), sequenced using the ABI Prism 3100 genetic analyzer (Applied Biosystems, USA) and subcloned into the EcoRI and XhoI sites of the mammalian expression vector, pcDNA.3.1/myc-His(-) B (pCDB) (Invitrogen), and the pEGFP-N1 expression vector (Clontech).

Hep2 cells were cotransfected with DCUN1D5-pEGFP-N1 and an endoplasmic reticulum-specific plasmid (donated by Peking University, China). After a 24-h incubation, cells were stained with 4', 6-diamidino-2-phenylindole (DAPI) and imaged by immunofluorescence microscopy (IX71-141, Olympus, Japan).

#### Ultraviolet C (UVC) exposure

HeLa cells grown to 60% to 80% confluence in 6-well plates were washed twice in phosphate-buffered saline (PBS) and then overlaid with 2 ml of PBS at 37 °C. The lids were removed and the cells were exposed to UVC light (254 nm) at a dose of 40 J/m<sup>2</sup> for 10 min, 40 J/m<sup>2</sup> for 15 min, 80 J/m<sup>2</sup> for 10 min, and 80 J/m<sup>2</sup> for 15 min. The

medium was then replaced, and the cells were harvested at 0, 24, or 48 h for in vitro analysis.

#### Western blot analysis

Whole cell protein extracts were prepared in RIPA lysis buffer. Equal amounts of cell lysates were added with 5 x Tris-glycine sodium dodecyl sulfate (SDS) sample buffer, subjected to electrophoresis on an SDS/15% polyacrylamide gel, and transferred to a nitrocellulose membrane (Amersham Pharmacia, UK). Proteins were detected with use of monoclonal rabbit anti-DCUN1D5 antibody (1:1000, Protein Tech Inc., China). The blots were scanned with use of the Odyssey Imaging System (LI-COR Bioscience, USA). The expression of  $\beta$ -actin protein was used as a control.

#### Wound healing assay

Hep2 cells were seeded in 6-well plates at a density of 100,000 cells per well and grown to a monolayer. A scratch in the monolayer was made using a 10- $\mu$ l pipette tip. The debris was washed away with PBS, and cells were incubated in serum-free medium. Cells of same regions along the wound area were imaged at 0, 24, and 48 h. Inverted fluorescence microscopy (IX71-141, Olympus, Japan) was used to identify the average width of the area devoid of cells.

#### Matrigel invasion assay

Hep2 cell invasion was quantified with use of a BD Matrigel Invasion Chamber fitted with an 8.0- $\mu$ m PET membrane (BD Biosciences). The membrane was soaked in RPMI 1640 medium and incubated at 37 °C for 2 h. The bottom well contained high-glucose RPMI 1640 medium containing 5% FBS. Cells were added to the upper well and incubated in serum-free medium. After 24 h of incubation, the cells on the upper surface were removed by wiping with a cotton swab. The membrane was stained with hematoxylin and eosin, and cell invasion was determined by counting 10 randomly selected fields.

#### Colony formation assay

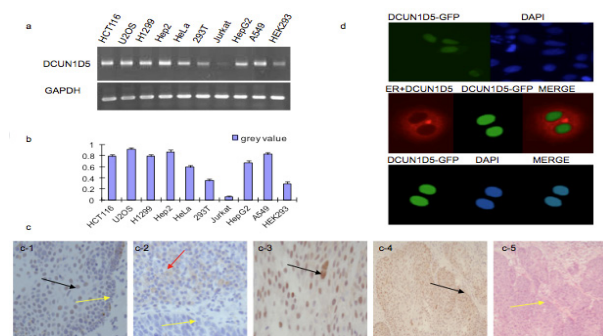
Hep2 cells were plated in 6-cm dishes at 2 x 10<sup>4</sup> cells/cm<sup>2</sup> and transfected with DCUN1D5, pCDB, and H-RAS separately. Cells were then harvested by trypsinization after incubation of 24 h and replated in 6-well plates at a density of 5 x 10<sup>2</sup> cells/ml. After 2 weeks of G418 selection (500  $\mu$ g/ml), colonies were fixed, stained with crystal violet, and counted.

#### Cell cycle and apoptosis analysis

HeLa cells were grown in 6-well plates to 60% confluence and transiently transfected with siRNAs at a final concentration of 100 nM. Cells were collected at 24 h after post-transfection and washed twice with PBS. For cell apoptosis measurement, cells were resuspended in 1x binding buffer, and 5  $\mu$ l of annexin fluorescein isothiocyanate (FITC) conjugate and 10  $\mu$ l of propidium iodide (50  $\mu$ g/ml) solution were added to each cell suspension, separately. For cell cycle analysis, the cells were fixed in 70% ethanol overnight at 4°C and were resuspended in staining solution (50  $\mu$ g/ml of propidium iodide, 1 mg/ml of RNase A, and 0.1% Triton X-100

**Table 1. Twenty Most Differentially Expressed Genes from Microarray Data**

Oligo ID	Gene ID	Gene Name	Refseq	GeneBank Accession	GO-biological_process	GO-molecular_function
H200004472	26585	GREM1	NM_01337	AY232290	0009653:morphogenesis	0005488:binding
H200005017	25818	KLK5	NM_01242	AY359010	0007275:development	0004295:trypsin activity
H200002586	6362	CCL18	NM_002988	Y13710	0016064:humoral defense mechanism	0005125:cytokine activity
H200019767	3854	KRT6B	NM_005555	—	0005200:integrity of a cytoskeletal	0007398:ectoderm development
H200019973	94240	EPSTI1	NM_033255	AL831953	—	tumor microenvironment
H200005753	79716	NPEPL1	NM_024663	AB075854	0019538: protein metabolism	0046872:metal ion binding
H200005848	79412	KREMEN2	NM_024507	BC009383	0007154: cell communication	—
H200000220	9636	ISG15	NM_005101	M13755	—	0042296: ligase activity
H200000695	1001	CDH3	NM_001793	X63629	0050953:sensory perception of light	0005515:protein binding
H200012063	3861	KRT14	NM_000526	BC042437	0007275:development	0005200:structural constituent of cytoskeleton
H200016555	2537	G1P3	NM_022873	—	0006950:response to stress	—
H200010239	1515	CTSL2	NM_001333	BC067289	0019538:protein metabolism	0004175:endopeptidase activity
H200005931	84259	DCUN1D5	NM_032299	NC000011	—	—
H200019493	3853	KRT6A	NM_005554	BC014152	0005200:integrity of a cytoskeletal	0007398:ectoderm development
H200005329	53836	GPR87	NM_023915	AK027784	0007154:cell communication	0016502:nucleotide receptor activity
H200011190	400961	Q9ULR5	NM_376062	AB032981	—	0030371:translation repressor activity
H200015640	2273	FHL1	NM_001449	AK122708	0030154:cell differentiation	—
H200014099	1675	DF	NM_001928	M84526	0006950:response to stress	0004295:trypsin activity
H200014995	5284	PIGR	NM_002644	AK026320	0046903:secretion	0005215:transporter activity
H200005487	92304	SCGB3A1	NM_052863	—	0008283:cell proliferation	0004871:signal transducer activity

**Figure 1. DCUN1D5 mRNA Transcription Across Multiple Cell Lines and Protein Localization.**

(a) Endogenous expression of DCUN1D5 was analyzed in ten human cell lines by RT-PCR. (Note: HCT116, human colonic epithelial cell line; U2OS, human osteosarcoma cell line; HepG2, human hepatocellular liver carcinoma cell line; A549, human lung adenocarcinoma epithelial cell line; H1299, human non-small cell lung carcinoma cell line; Jurkat, human T cell lymphoblast-like cell line; HEK293, human embryonic kidney cell line; and 293T, transformed human embryonic kidney cell line). (b) Densitometric analysis of RT-PCR results showed in (a), and data (mean  $\pm$  SD) represented from three independent experiments. (c) Immunohistochemical analysis of DCUN1D5 in primary LSCC tissue samples. Panels c-1, c-2 and c-3 show 400 $\times$ magnification; panels c-4 and c-5 show 100 $\times$ magnification. Black arrows denote cells staining positive nuclear DCUN1D5 immunoreactivity; Yellow arrows denote squamous cancer cells; and Red arrow denotes plasmas cells staining positive for DCUN1D5. Panel c-5 showed the corresponding hematoxylin and eosin (H&E) stain. (d) Hep2 cells were transfected with DCUN1D5-pEGFP-N1 or endoplasmic reticulum tagged plasmid plus DCUN1D5-pEGFP-N1 and images were captured at 24h

in PBS). Cells were then analyzed by the fluorescence activated cell sorting (FACS) method. DNA content per cell was measured with use of the CellQuest Pro program (Becton Dickinson).

#### Statistical analysis

Data were reported as mean  $\pm$  SD or as median (range). Each experiment was repeated at least three

times. Statistical significance of the differences between experimental groups was determined by Student's t test. The  $\chi^2$  test was used to evaluate the differences in the distributions of selected demographic characteristics between DCUN1D5 positive and DCUN1D5 negative cases. All analyses were two sided. Values of  $p < 0.05$  were considered statistically significant.

## Results

### Genomic gene expression sequence analysis and prediction

Differential patterns in gene expression between five paired LSCC samples and paired normal tissues were determined based on the average log ratios. Among the 20 highest-ranked genes from microarray data (Table 1), DCUN1D5 was the only gene whose function was not yet known.

DCUN1D5 protein (NP\_115675) contained two domains, including a DCN1 domain, which was a scaffold-like E3 ligase for cullin neddylation that displayed ubiquitin ligase activity, and a DUF298 domain of unknown function. Members of the DUF family contained a basic helix-loop-helix leucine zipper motif, which was implicated in some aspects of neddylation of the cullin 3 family and had a possible role, along with the DCN1 domain, in the regulation of DNA repair and cell cycle progression (Kurz et al., 2005; Yang et al., 2007).

### DCUN1D5 expression in human cancer cell lines

RT-PCR was performed to identify the transcriptional level of DCUN1D5 in 10 human cancer cell lines (Fig. 1a). Semi-quantitative results revealed that the relative expression levels of DCUN1D5 differed across various cell lines. Normalization of the data to GAPDH indicated that DCUN1D5 was moderately to highly expressed in Hep2 and HeLa cells (Figure 1b).

### DCUN1D5 overexpression in primary LSCC tissues

The correlations between DCUN1D5 expression and

**Table 2. Characteristics of 50 Patients with LSCC**

Variable	Total (No. = 50)		DCUN1D5 positive staining (No. = 12)		DCUN1D5 negative staining (No. = 38)		P value*
	No.	%	No.	%	No.	%	
	Age						
≤ 50 years	9	18	2	16.7	7	18.4	
> 50 years	41	82	10	83.3	31	81.6	
Sex							1
Male	46	92	11	91.7	35	92.1	
Female	4	8	1	8.3	3	7.9	
Tobacco smoking							0.32
Ever	45	90	12	100	33	86.8	
Never	5	10	0	0	5	13.2	
Alcohol drinking							1
Ever	30	60	7	58.3	23	60.5	
Never	20	40	5	41.7	15	39.5	
Histology							0.42
Precancerous lesions	10	20	1	8.3	9	23.7	
Squamous cell carcinoma	40	80	11	91.7	29	76.3	
TNM stage							0.5
I or II	18	36	3	25	15	39.5	
III or IV	32	64	9	75	23	60.5	

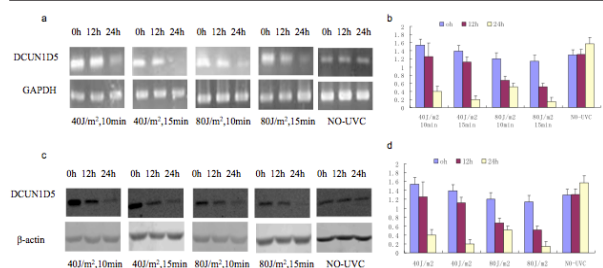


**Figure 2. DCUN1D5 Gene and Protein Expression in HeLa Cells After UVC Treatment.** (a) RT-PCR analysis of DCUN1D5 mRNA expression after 40J/m<sup>2</sup> for 10 and 15min, 80J/m<sup>2</sup> for 10 and 15min UVC exposures, respectively, and cells were harvested at 0, 12 and 24h post exposure. (b) Densitometric analysis of RT-PCR results from (a), and data (mean ± SD) represented from three independent experiments. (c) Western blot detection of DCUN1D5 protein expression in HeLa cells after the same UVC exposure. (d) Densitometric analysis of Western blot results from (c) and data (mean ± SD) represented from three independent experiments

age, sex, smoking, alcohol use, histology, and cancer staging among 50 LSCC patients were shown in Table 2. DCUN1D5 protein was overexpressed in 12 (24.0%) of 50 squamous epithelial cancerous tissue samples from 50 LSCC patients and negative expressed in all paired noncancerous normal tissues. 40 primary LSCCs and 10 precancerous lesions were analyzed in all, resulting in the detection of positive nuclear DCUN1D5 immunoreactivity in 11 (27.5%) LSCCs and 1 (10.0%) precancerous lesion, respectively (Table 2). Moreover, all of the patients with positive LSCCs had a smoking history. No differences in DCUN1D5 immunoreactivity were observed between different tumor-node-metastasis (TNM) stages ( $p = 0.50$ ) or histologic subgroups ( $p = 0.42$ ). We found that endogenous DCUN1D5 localized to the nucleus in squamous epithelial cancerous tissues (Figure 1c1-4). Pathology was confirmed in all samples by hematoxylin and eosin staining (Figure 1c-5). Interestingly, we observed DCUN1D5-positive plasma cells surrounding the epithelial cells in 5 LSCC patients (Figure 1c-2).

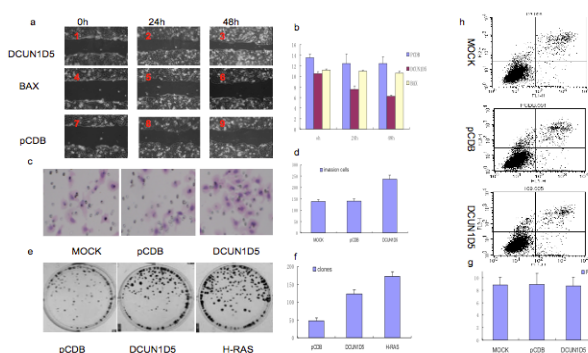


**Figure 3. Effect of Overexpression of DCUN1D5 on the Migration, Invasion, Proliferation and Apoptosis in Hep2 Cells.** (a) Representative image of wound assay shows cell migration into denuded wound area (×200) at 0, 24, and 48 h. 1-3: migration of cells over-expressing DCUN1D5; 4-6: migration of cells over-expressing BAX as a negative control; and 7-9: migration of cells transfected with pCDB as a vector control. (b) Data (mean ± SD) expressed as width of cells migrated to wound area from three independent experiments. (c) Invasion assays were performed and cells invaded through the membrane were analyzed. MOCK: no transfection as a normal control and pCDB: a vector control. (d) Data (mean ± SD) expressed as numbers of invaded cells from three independent experiments. (e) Colony formation analysis of cell proliferation. pCDB: a vector control and H-RAS: a positive control. (f) Quantification of colony formation. (g) The percentage of apoptotic cells were analyzed by FACS. MOCK: no transfection as a normal control and pCDB: a vector control. (h) Data (mean ± SD) represented the mean value of the three independent apoptosis experiments

#### Subcellular localization of DCUN1D5

Similar to the results of immunohistochemistry in squamous epithelial cancerous tissues (Figure 1c), subcellular localization analysis indicated that endogenous DCUN1D5 localized to the nucleus in Hep2 cells (Figure 1d) and HeLa cells.

#### UVC exposure reduced endogenous DCUN1D5 expression

RT-PCR analysis showed that endogenous expression of DCUN1D5 decreased in a time-dependent manner after UVC treatment (Figure 2a, b). Western blot analysis was performed to determine DCUN1D5 protein levels at 0, 12 and 24 h intervals. Endogenous DCUN1D5 protein expression was also decreased in a time-dependent manner after UVC exposure (Figure 2c, d).

#### Overexpression of DCUN1D5 increased cell migration, invasion, and proliferation in vitro, but not apoptosis

A wound healing assay was performed to detect the migration ability of Hep2 cells. Phase-contrast microscopy imaging revealed that overexpression of DCUN1D5 resulted in 2.7 times greater migration to the wound area at 24 h compared with the pCDB-treated controls (Figure 3a, b).

A Matrigel invasion assay was used to investigate the role of DCUN1D5 in cell invasion. Overexpression of DCUN1D5 protein resulted in increased Hep2 cells invasion, as the number of cells proceeded through the membrane increased by 67.5% compared with the pCDB-treated (Figure 3c, d).

Further, a colony formation assay was performed to

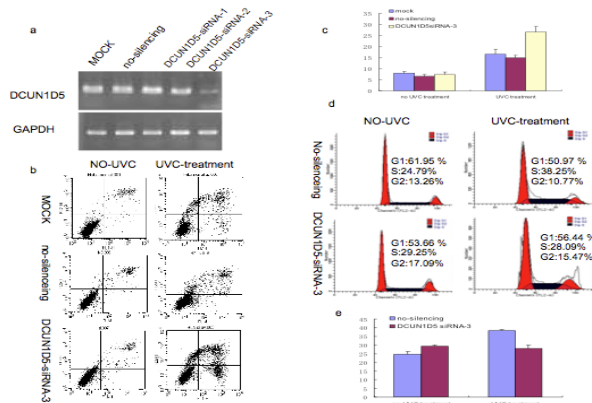


**Figure 4. Effect of Inhibition of the Endogenous DCUN1D5 Expression on Apoptosis and Cell Cycle Progression in HeLa Cells Following UVC Exposure.**

(a) Screening of siRNA directed against DCUN1D5 and the siRNA effects were determined by RT-PCR. (b) Cells after 12h transfection of DCUN1D5-siRNA-3 were irradiated with 80 J/m<sup>2</sup> UVC for 15min and harvested 24 h thereafter for apoptosis analysis. MOCK panel: no transfection as a normal control and no-silencing panel: a vector control. (c) Data (mean  $\pm$  SD) indicated apoptosis values from three independent experiments. (d) 24 h after treatment with 80 J/m<sup>2</sup> UVC for 15 min or mock treated, cells were collected and analyzed for cell cycle profile. The percentage of cells in G1, S, and G2 phases was shown. (e) The cells in S stage (% of total) were shown in bar graph. Data (means  $\pm$  SD) indicated from three independent experiments

determine the impact of DCUN1D5 expression on Hep2 cells proliferation. Significantly larger colonies were observed following overexpression of DCUN1D5, and 2.6 times more colonies were quantified compared with the pCDB-treated controls (Figure 3e, f).

To determine the impact of DCUN1D5 expression on apoptosis, Hep2 cells were harvested 24 h after transfection, and apoptosis was analyzed by the FACS method. Data indicated that the percentage of apoptotic cells did not differ significantly between cells overexpressing DCUN1D5 and controls (Figure 3g, h).

#### *Knockdown of DCUN1D5 blocked S phase progression and increased apoptosis after UVC irradiation in vitro*

The DCUN1D5-siRNA-3 was identified and chosen for subsequent knockdown studies, because DCUN1D5 mRNA was significantly decreased 24 h after transfection in HeLa cells (Figure 4a). Cell cycle results indicated that DCUN1D5-siRNA-3 decreased the number of cells in the S phase by 10.2% compared with controls after UVC treatment, whereas the number of cells in the S phase increased by 4.5% without UVC exposure (Figure 4b, c). Similarly, DCUN1D5-siRNA-3-treated cells displayed an 11.7% increase in apoptosis compared with controls after UVC treatment, whereas the number of apoptosis cells increased by 0.9% without UVC exposure (Figure 4d, e).

## Discussion

Smoking is a primary risk factor for laryngeal carcinogenesis because chemicals in cigarette can modify and mutate DNA (Khlifi et al., 2010; Mallis et al., 2011). Neoplasms induced by tobacco smoking have more

complex etiology because of the presence of various carcinogenic agents (Slebos et al., 2002; Hang B, 2010). High-density microarray expression profiling can be a valuable tool for identifying putative genes involved in critical cellular activities (Chung et al., 2004; Chen et al., 2010).

We utilized microarray analysis to identify DCUN1D5, a UVC-responsive gene that affected cell cycle progression and apoptosis following genotoxic shock. Overexpression of DCUN1D5 promoted the proliferation, migration, and invasion in vitro, with no impact on apoptosis. After exposure to UVC irradiation, endogenous DCUN1D5 expression decreased in a time-dependent manner. Moreover, siRNA silencing of DCUN1D5 decreased the number of cells in the S phase and increased apoptosis after UVC exposure. To our knowledge, these data are the first to identify a role of DCUN1D5 contributing to SCC progression. Further, these data suggest that DCUN1D5 may have a vital function involved in DNA damage response and provide new clues to yet-unknown signal transduction pathways activated by genotoxic stress.

Useful hints about the function of DCUN1D5 can also be found with the help of bioinformatic tools. Motif analysis (Chen et al., 2009; Eisenhaber et al., 2010) in the MnM database (Minimotif Miner 2.4) indicated that there were three putative binding sites for DNA damage response proteins such as ATM (ataxia-telangiectasia mutated) and ATR (ataxia-telangiectasia and Rad3-related). Additionally, there was a putative Rad53 binding site. Recently, researchers uncovered a novel MEC1-RAD53-DCN1-dependent signaling pathway that prevented deleterious DSB-specific telomerase additions at DNA breaks, thus preserving genomic integrity (Makovets et al., 2009; Kurz et al., 2008). Taken together, these findings suggested that the DCUN1D5 might play a role in DNA damage response to genotoxic stress and probably subsequent DNA repair. These data were consistent with what we found in cell lines, specifically, that DCUN1D5 had distinct phenotypes and exhibited responsiveness to DNA damage.

UVC irradiation (<280 nm) caused direct DNA photodamage by inducing cyclobutane pyrimidine dimers that were associated with mutagenesis and tumorigenesis (Pfeifer et al., 2005). DNA damage following UVC exposure induced G1/S cell cycle arrest (Gentile et al., 2003). Therefore, the UVC model was chosen to investigate the role of DCUN1D5 in DNA damage response. In our study, we found that siRNA knockdown of endogenous DCUN1D5 expression decreased the percentage of cells in the S phase and increased the percentage of cells undergoing apoptosis after UVC treatment. In contrast, we did not detect any effect of DCUN1D5 on apoptosis in cells that were not exposed to UVC, which suggested that DCUN1D5 might block cell cycle progression to facilitate the repair of damaged DNA. We speculated that DCUN1D5 could have similar roles in DNA repair following cigarette smoke-induced genotoxic stress. However, the precise mechanisms involved in the function of DCUN1D5 in the cell cycle, cell survival, and cell growth require further investigation.

Another interesting result of immunohistological analysis revealed that DCUN1D5 was expressed in plasma cells surrounding the epithelial cells. This finding suggested that DCUN1D5 might be involved in host immune response in LSCC. Because the immune system mounted a defense against cancer development and the persistent inflammatory reactions facilitated tumor progression (Bhutia et al., 2010; Gomes et al., 2010), there was no clear understanding of the immune response in the development of LSCC. Hahne et al reported that melanoma cells bore Apo-1 or Fas on their surfaces, which induced immune cells to initiate apoptosis (Hahne et al., 1996). The hypothesis that DCUN1D5 may play a role in host immune responses inducing apoptosis needs further study.

Our data describe, for the first time, a role of DCUN1D5 in DNA damage response in vitro. Further studies are needed to elucidate the mechanisms behind the roles of DCUN1D5 involved in DNA damage and repair, for correlations of such findings with additional clinical parameters and prognosis are warranted.

## Acknowledgements

This work was supported by awards from National Science Foundation to Z.H. (#30973293); a grant from Capital Development Fund for medical research to Z.H. (#2007-2065).

## References

- Bhutia SK, Mallick SK, Maiti TK (2010). Tumour escape mechanisms and their therapeutic implications in combination tumour therapy. *Cell Biol Int*, **34**, 553-63.
- Cavaliere D, Dolara P, Mini E, et al (2007). Analysis of gene expression profiles reveals novel correlations with the clinical course of colorectal cancer. *Oncol Res*, **16**, 535-48.
- Chen L, Xuan J, Wang C, et al (2009). Biomarker identification by knowledge-driven multilevel ICA and motif analysis. *Int J Data Min Bioinform*, **3**, 365-81.
- Chen SH, Albuquerque CP, Liang J, Suhandynata RT, Zhou H (2010). A proteome-wide analysis of kinase-substrate network in the DNA damage response. *J Biol Chem*, **285**, 12803-12.
- Chung CH, Parker JS, Karaca G, et al (2004). Molecular classification of head and neck squamous cell carcinomas using patterns of gene expression. *Cancer Cell*, **5**, 489-500.
- Curado MP, Hashibe M (2009). Recent changes in the epidemiology of head and neck cancer. *Curr Opin Oncol*, **21**, 194-200.
- Eisenhaber B, Eisenhaber F (2010). Prediction of posttranslational modification of proteins from their amino acid sequence. *Methods Mol Biol*, **609**, 365-84.
- Gentile M, Latonen L, Laiho M (2003). Cell cycle arrest and apoptosis provoked by UV radiation-induced DNA damage are transcriptionally highly divergent responses. *Nucleic Acids Res*, **31**, 4779-90.
- Gomes CP, Freire MS, Pires BR, et al (2010). Comparative proteomic and metalloproteomic analyses of human plasma from patients with laryngeal cancer. *Cancer Immunol Immunother*, **59**, 173-81.
- Hahne M, Rimoldi D, Schröter M, et al (1996). Melanoma cell expression of Fas(Apo-1/CD95) ligand: implications for tumor immune escape. *Science*, **274**, 1363-6.
- Hang B (2010). Formation and repair of tobacco carcinogen-derived bulky DNA adducts. *J Nucleic Acids*, e709521.
- Hermesen M, Alonso Guervós M, Meijer G, et al (2005). Chromosomal changes in relation to clinical outcome in larynx and pharynx squamous cell carcinoma. *Cell Oncol*, **27**, 191-8.
- Khlifi R, Hamza-Chaffai A (2010). Head and neck cancer due to heavy metal exposure via tobacco smoking and professional exposure: a review. *Toxicol Appl Pharmacol*, **248**, 71-88.
- Kurz T, Ozlü N, Rudolf F, et al (2005). The conserved protein DCN-1/Dcn1p is required for cullin neddylation in *C. elegans* and *S. cerevisiae*. *Nature*, **435**, 1257-61.
- Kurz T, Chou YC, Willems AR, et al (2008). Dcn1 functions as a scaffold-type E3 ligase for cullin neddylation. *Mol Cell*, **29**, 23-35.
- Leemans CR, Braakhuis BJ, Brakenhoff RH (2011). The molecular biology of head and neck cancer. *Nat Rev Cancer*, **11**, 9-22.
- Makovets S, Blackburn EH (2009). DNA damage signalling prevents deleterious telomere addition at DNA breaks. *Nat Cell Biol*, **11**, 1383-1386.
- Mallis A, Jelastopulu E, Mastronikolis NS, et al (2011). Laryngeal cancer and passive smoking: the neglected factor? *Eur Arch Otorhinolaryngol*, **268**, 727-31.
- Moktar A, Singh R, Vadhanam MV, et al (2011). Cigarette smoke condensate-induced oxidative DNA damage and its removal in human cervical cancer cells. *Int J Oncol*, **39**, 941-7.
- Parikh RA, White JS, Huang X, et al (2007). Loss of distal 11q is associated with DNA repair deficiency and reduced sensitivity to ionizing radiation in head and neck squamous cell carcinoma. *Genes Chromosomes Cancer*, **46**, 761-75.
- Pfeifer GP, Denissenko MF, Olivier M, et al (2002). Tobacco smoke carcinogens, DNA damage and p53 mutations in smoking-associated cancers. *Oncogene*, **21**, 7435-51.
- Pfeifer GP, You YH, Besaratinia A (2005). Mutations induced by ultraviolet light. *Mutat Res*, **571**, 19-31.
- Rajkumar T, Vijayalakshmi N, Sabitha K, et al (2009). A 7 gene expression score predicts for radiation response in cancer cervix. *BMC Cancer*, **9**, 365.
- Slebos RJ, Oh DS, Umbach DM, Taylor JA (2002). Mutations in tetranucleotide repeats following DNA damage depend on repeat sequence and carcinogenic agent. *Cancer Res*, **62**, 6052-60.
- Tusher VG, Tibshirani R, Chu G (2001). Significance analysis of microarrays applied to the ionizing radiation response. *Proc Natl Acad Sci USA*, **98**, 5116-21.
- Yang X, Zhou J, Sun L, et al (2007). Structural basis for the function of DCN-1 in protein Neddylation. *J Biol Chem*, **282**, 24490-4.
- Zhong Q, Guo W, Chen X, et al (2011). Rhinoscleroma: a retrospective study of pathologic and clinical features. *J Otolaryngol Head Neck Surg*, **40**, 167-74.
- Zhou X, Jordan RC, Li Y, Huang BL, Wong DT (2005). Frequent allelic imbalances at 8p and 11q22 in oral and oropharyngeal epithelial dysplastic lesions. *Cancer Genetics and Cytogenetics*, **161**, 86-9.